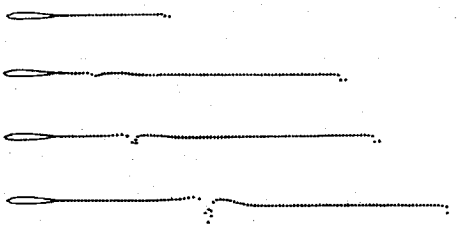

Fig. 1 Vortical wake predicted by vortical flow analysis.

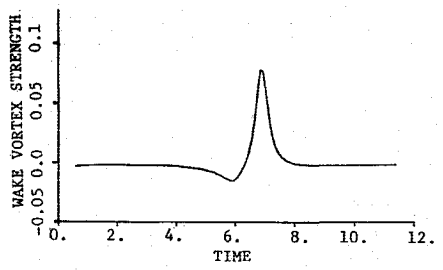

Fig. 2 Time history of vortex shedding.

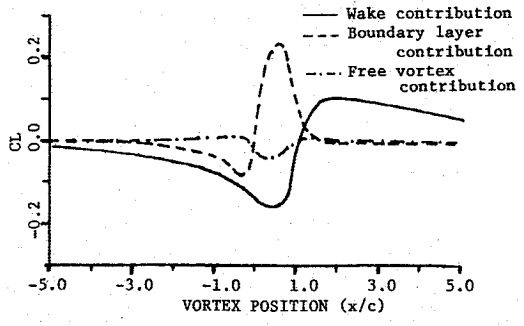

Fig. 3 Unsteady lift components predicted by vortical flow analysis.

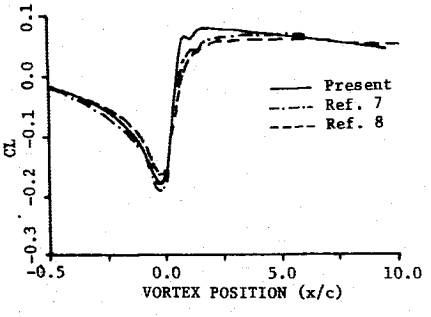

Fig. 4 Unsteady lift compared with transonic flow solution.

edge, and the flow picture would be distorted. Figure 2 shows the strengths of the wake vortices plotted against the time. In Fig. 3, the unsteady lift components induced by the three vortical regions are plotted separately. These curves show that the most important factor in this blade-vortex interaction is the vortex shedding process. Figure 4 shows the total vortex-induced unsteady lift as compared to the viscous flow solutions given by McCroskey and Goorjian[7] and by Sankar and Tang.[8] The good agreement between the present results and those of others from viscous flow solvers indicates that the present vortex flow model simulates high-Reynolds number attached unsteady flows very accurately.

Conclusion

A vortex flow model for the problem of two-dimensional blade-vortex interaction has been established, and closed-form solutions for the vortex-induced unsteady force are derived. A new trailing-edge flow model (unsteady Kutta condition) is introduced; this trailing-edge flow model is physically more meaningful than the conventional stagnation point method. It has been established that the present approach can accurately predict the vortex-induced unsteady force without tedious computations.

References

[1]Fink, P. T. and Soh, W. K., "Calculation of Vortex Sheets in Unsteady Flow and Applications in Ship Hydrodynamics," *Proceedings of the 10th Symposium on Naval Hydrodynamics,* Cambridge, MA, 1974.

[2]Basu, B. C. and Hancock, G. J., "The Unsteady Motion of a Two-Dimensional Aerofoil in Incompressible Inviscid Flow," *Journal of Fluid Mechanics,* Vol. 87, 1978, pp. 159–178.

[3]Poling, D. R. and Telionis, D. P., "The Response of Airfoils to Periodic Disturbances—The Unsteady Kutta Condition," *AIAA Journal,* Vol. 24, Feb. 1986, pp. 193–199.

[4]Wu, J. C., "Theory for Aerodynamic Forces and Moments," *AIAA Journal,* Vol. 19, April 1981, pp. 432–441.

[5]Wu, J. C. and Hsu, T. M., "The Unsteady Forces and Moments Induced by Blade-Vortex Interaction," *Proceedings of AHS Specialists' Meeting on Aerodynamics and Aeroacoustics,* Arlington, TX, 1987.

[6]Hsu, T. M., "Theoretical and Numerical Studies of a Vortex-Airfoil Interaction Problem," Ph.D. Thesis, Georgia Institute of Technology, 1986.

[7]McCroskey, W. J. and Goorjian, P. M., "Interactions of Airfoils with Gusts and Concentrated Vortices in Unsteady Transonic Flow," AIAA Paper 83-169, July 1983.

[8]Sankar, N. L. and Tang, W., "Numerical Solution of Unsteady Viscous Flow Past Rotor Section," AIAA Paper 85-0129, Jan. 1985.

Recirculation Structure of the Coannular Swirling Jets in a Combustor

Y. C. Chao*
National Cheng Kung University, Tainan, Taiwan, Republic of China

Introduction

SWIRL is used extensively in gas turbine combustors to achieve high-combustion efficiency, stable combustion over a wide range of operation, good temperature transverse quantity, and minimum size. In the study of swirling flows, the term "vortex breakdown" refers to the formation of a recirculation zone on the axis of flow.[1] The swirl-induced recirculation zone is an important phenomenon of combustor research.

Previous experiments and computations[2–4] have focused upon single or multiple swirling jets generated by swirl tubes in combustors. Recently, So et al.[5] observed that the swirling flowfield generated by vane swirler possesses two recirculation regions in the center of the test model, one very close to the swirler hub and one further downstream. They could not explain the reason why there are two recirculations coexisting. Due to the fact that the first recirculation is very small compared to the second, and the axial velocity between these two

Presented in part as Paper 87–0305 at the AIAA 25th Aerospace Science Meeting, Reno, NV, Jan. 12–15, 1987; received May 8, 1987; revision received Nov. 23, 1987.

*Associate Professor, Institute of Aeronautics and Astronautics. Member AIAA.

recirculations is low, they attributed this phenomenon to experimental error. However, we believe that the first recirculation is strongly related to the central hub. In order to examine this phenomenon and to closely simulate the double-swirler arrangement[6] in a modern combustor, in this Note swirl is generated by two coannular vane swirlers located at the entrance, with a central hub in the location of the fuel injector in an actual combustor (see Fig. 1). The relative direction of the swirl imparted to the two jets in a coannular configuration, together with the possible wake flow phenomenon due to the central hub, will affect the recirculation structure in a very complicated manner.

Experiments

The overall experimental setup consists of a blower (7.5 Hp), a settling chamber, two sets of annular vane swirlers, and a model combustor test section (see Fig. 1). A five-hole pitot probe is employed to measure the mean velocity, static pressure, and flow direction for this complicated three-dimensional. (A five-hole pitot probe has been successfully used as a three-dimensional measuring tool in swirling flow problems.)[3,7] Two sets of experiments are performed. The first set (Cases A, B, C, D, and E in Table 1) starts from the maximum counterswirl condition, with the magnitude of the outer swirl gradually decreased until the maximum coswirl condition is reached. The second set of experiments (Cases G, A, E, and F in Table 1) is similar to the first one, except that the magnitude of the inner swirl is decreased. Variations in the inlet Reynolds number, based on maximum inlet axial velocity $U_{in} = 30$ m/s and inlet diameter, lie between 2×10^5 and 2.5×10^5.

The overall swirl intensity issued from the double-swirler can be characterized by the swirl number $S = G_\phi/(G_x R)$, according to Beér and Chigier,[8] where R is the swirler exit radius and G_ϕ and G_x are the axial flux of angular and axial momenta, respectively. The absolute values of the swirl numbers for various inner and outer swirler arrangements are shown in Table 1. The swirl number sequence in decreasing order is the following: cases F, E, A, G, D, B, and C.

Results and Discussion

Results of the measured axial velocity component of case E and the reversed flow regions of the first set of experiments are shown in Fig. 2. The dotted line in the axial velocity plot is the locus of the zero axial components which indicates the reversed flow regions. Case E ($S = 0.55$) presents the typical flowfield of the strong swirl flow. For strong swirl flows, the central vortex breakdown occurs and, due to the presence of the strong swirl-induced adverse pressure gradient,[3] the central vortex breakdown moves upstream and stabilizes itself at the swirler hub. No corner recirculation zone is observed. The tangential velocity distribution[9] develops into Rankin vortex[8] in the region $x/D > 1.0$, corresponding to the region immediately downstream of the recirculation zone. On the other hand, case D ($S = 0.33$) shows the characteristics of the weak swirl flow: central vortex breakdown may (this case) or may not (cases B and C with lower swirl number) occur, the central vortex breakdown is stabilized in the middle of the test section, corner recirculation zone is notable, and there is no obvious Rankin vortex for tangential component distribution.[9] Apparently, cases B, C, and D belong to the weak swirl flow category and cases G, A, E, and F belong to the strong swirl flow.[9] Case C, 15 deg inner and 0 deg outer vane angles and $S = 0.032$, is the lowest swirl number case that is very similar to the nonswirl parallel jet over a central hub. The central recirculation region is close to the hub and extends only to $x/D = 0.17$, which is very close to the size of the nonswirl wake bubble. The development of the axial velocity component (not shown) in the test section resembles the nonswirl parallel jet. As the swirl number is increased in case B ($S = 0.27$), the central wake bubble is elongated to $x/D = 0.35$. The swirl number is further increased in case D; the size of the reversed flow region is first reduced at $x/D = 0.3$ and then increased to become another bubble. The bottleneck-like shape of the reversed flow region is believed to consist of two recirculation zones of different characteristics; one is the separation wake bubble generated by the hub, the other is the recirculation zone due to the swirling vortex breakdown. For strong swirl cases of G, A, E, and F, the shape and size of the reversed flow regions look almost the same, except that the thickness of the tail is different.[9] A question arises naturally: in the cases of high swirl strength, does the central recirculation zone possess two cells? To investigate the detailed structure of the central recirculation zone, fine measurement of the velocity is made in the near-hub region. The resultant U-V flow direction at each measurement station (in order to avoid possible schematic confusion, the magnitude of the U-V velocity is not shown) is shown in Fig. 3 for cases D and E. Again the dotted lines in-

Table 1 Flow arrangements

	A	B	C	D	E	F	G
Inner vane angle deg	−15	−15	−15	−15	−15	-45	−45
Outer vane angle deg	45	30	0	−30	−45	−45	45
Swirl no. |S|	0.49	0.27	0.032	0.33	0.55	0.64	0.4

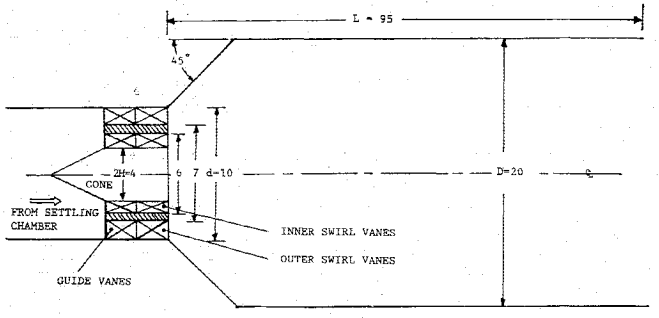

Fig. 1 Test section geometry (dimensions in cm).

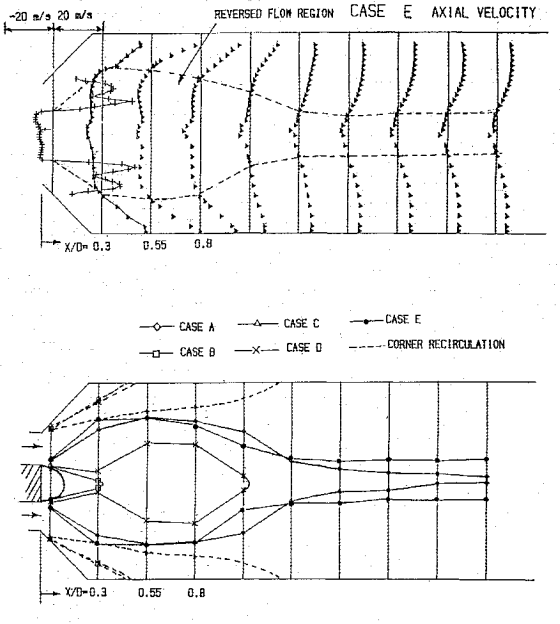

Fig. 2 Axial velocity component of typical strong swirl flow case E and the reversed flow regions of cases A, B, C, D, and E.

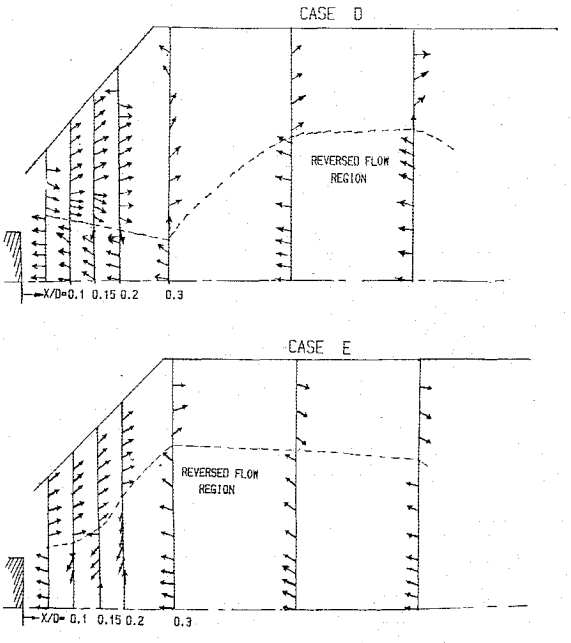

Fig. 3 Flow directions on the symmetric plane of cases D and E.

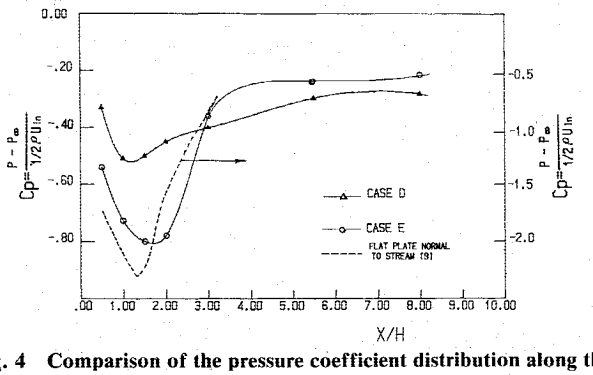

Fig. 4 Comparison of the pressure coefficient distribution along the central axis of cases D and E and the case of flow behind a flat plate normal to the stream.

dicate the reversed flow regions. It is obvious that case D has two cells, with the first smaller cell oriented downward toward the central axis. Due to swirling vortex breakdown, the second cell is parallel to the axis. Thus, these two cells stabilize each other and form a bottleneck-like shape of recirculation. Complicated unsteady flow is observed between the first and second cells. Surprisingly, case E also possesses two cells in the recirculation zone. However, unlike case D, the first smaller cell is oriented upward away from the central axis due to adverse pressure force. Flow between these two cells is complicated and unsteady. The distribution of center line pressure coefficient $C_p = (p - p_\infty)/(\rho U_{in}^2/2)$ of cases D and E, together with that of the flow behind a flat plate normal to stream,[10] are plotted in Fig. 4. The typical wake low pressure "trough" of the nonswirl wake bubble has also been noticed for both cases. The minimum static pressure is reached in $1 < x/H < 2$, and then the pressure is recovered in the "reattaching" region. Finally, the pressure reaches the plateau and the first recirculation is completed at $x/H = 3.0$, which corresponds to $x/D = 0.3$, the onset of the second cell in Fig. 4. Behind the plateau, the pressure shows a completely different trend, indicating different flow characteristics. This also confirms the conjecture of two-cell structure of the wake bubble and central vortex breakdown recirculation made above.

References

[1]Escudier, M. P. and Keller, J. J., "Recirculation in Swirling Flow: A Manifestation of Vortex Breakdown," *AIAA Journal,* Vol. 23, Jan. 1985, pp. 111–116.

[2]Habib, M. A. and Whitelaw, J. H., "Velocity Characteristics of Confined Coaxial Jets With and Without Swirl," *ASME Journal of Fluid Engineering,* Vol. 12, March 1980, pp. 47–53.

[3]Vu, B. T. and Gouldin, F. C., "Flow Measurements in a Model Swirl Combustor," *AIAA Journal,* Vol. 20, May 1982, pp. 642–651.

[4]Romas, J. I. and Somer, H. T., "Swirling Flow in a Research Combustor," *AIAA Journal,* Vol. 23, Feb. 1985, pp. 241–248.

[5]So, R. M. C., Ahmed, S. A., and Mongia, H. C., "Jet Characteristics in Confined Swirling Flow," *Experiments in Fluid,* Vol. 3, Aug. 1985, pp. 221–230.

[6]Lefebvre, A. W., *Gas Turbine Combustion,* 1st ed., McGraw-Hill, New York, 1983, p. 127.

[7]Rhode, D. L., Lilley, D. G., and McLaughlin, D. K., "Mean Flowfields in Axisymmetric Combustor Geometries with Swirl," *AIAA Journal,* Vol. 21, April 1983, pp. 593–600.

[8]Beér, J. M. and Chigier, N. A., *Combustion Aerodynamics,* Krieger Pub., Malabar, FL, 1983, pp. 106–112.

[9]Chao, Y. C., Ho, W. C., and Lin, S. K., "Experiments and Computations on the Coaxial Swirling Jets with Centerbody in an Axisymmetric Combustor," AIAA Paper 87-0305, 1987.

[10]Chang, P. K., *Separation of Flow,* Pergamon, Oxford, England, UK, 1970, pp. 335–350.

Solutions of One-Dimensional Steady Nozzle Flow Revisited

Meng-Sing Liou*
NASA Lewis Research Center, Cleveland, Ohio

Introduction

THE differential equations for one-dimensional steady nozzle flows are easily integrated to give equations connecting any two states of the flow considered. Despite the simplicity of their forms, little has been elaborated on the solutions of the equations in the literature.[1-5] In the discussion of the well-known pressure/Mach number distribution curves corresponding to varying back pressure in a divergent or convergent-divergent nozzle (Fig. 1), the proper parameters needed, and their functional relationship, are often obscured because it was not clear how the curve was constructed. Heretofore, to find loss of total pressure (and entropy increase) across a shock wave in a nozzle, one employed a trial and error procedure in which the shock wave location was iterated until the calculated exit pressure agreed with the specified value; then the change in total pressure immediately followed. Although the procedure is straightforward, it is nonetheless tedious and requires knowing the area distribution of the nozzle. Alternatively, a transcendental equation was solved via iteration or tabulation [pp. 211–212, Eq. (4.105) and Example 4.8 in Ref. 5]. The effect of the variables involved, however, is often buried.

In this paper we show a formulation which eliminates any iteration process for obtaining the entropy increase in the nozzle and leads to simple solution of a quadratic equation. Consequently, the proper parameters are explicitly seen in the equation and their effects on the solution are easily determined. Moreover, since only one root of the equation is physically admissible, it follows that the entropy production is uniquely determined. Hence, the shock wave is uniquely determined by this set of parameters. This point is particularly

Received May 8, 1987; revision received Nov. 6, 1987.

*Computational Fluid Dynamics Branch. Member AIAA.